Electrochemical Formation of Nd-Ni Alloys in Molten LiF-CaF$_2$-NdF$_3$

T. Nohira[a], S. Kobayashi[a], K. Kobayashi[a], R. Hagiwara[a], T. Oishi[b], and H. Konishi[c]

[a] Graduate School of Energy Science, Kyoto University
Sakyo-ku, Kyoto 606-8501, Japan
[b] National Institute of Advanced Industrial Science and Technology
Tsukuba, Ibaraki 305-8569, Japan
[c] Graduate School of Engineering, Osaka University
Suita, Osaka 565-0871, Japan

The electrochemical formation of Nd-Ni alloys was investigated in a molten LiF-CaF$_2$-NdF$_3$ (0.30 mol%) system at 1123 K. Cyclic voltammetry and open-circuit potentiometry indicated the formation of several phases of Nd-Ni alloys. The whole electrode became almost NdNi$_2$ phase by potentiostatic electrolysis of a 0.2 mm-thick Ni plate at 0.15 V vs. Li$^+$/Li for 75 minutes. The formed NdNi$_2$ electrodes were transformed to other phases such as NdNi$_3$ and NdNi$_5$. The existences of NdNi$_2$, NdNi$_3$ and NdNi$_5$ were confirmed by powder XRD analysis. By summarizing the results, the formation potential for each alloy phase has been determined.

Introduction

The use of rare earth (RE) elements in modern technology has increased dramatically over the past few decades. Thus, it is indispensable to develop an inexpensive and environment-friendly recovery/ separation process of the RE metals. Especially, the recovery of Nd and Dy from Nd-Fe-B magnet scraps will become a serious problem due to the widespread use of EV/HEV in the near future. From this background, the authors have proposed a new separation and recovery process of RE metals from scraps using molten salt and alloy diaphragm (1). This new process is based on our previous findings that a specific RE element forms selectively form alloys and also be dissolved from the alloys in molten salts (2). According to the study, Figure 1 shows the principle of molten salt electrochemical process using alloy diaphragm. A scrap metal containing RE metals is used as an anode. RE-IG metal alloy is used for the diaphragm as a bipolar electrode.

During the electrolysis, RE metals in the anode are dissolved into the molten salt as RE ions and they are reduced to form RE-IG metal alloy on the alloy diaphragm. Subsequently, RE atoms chemically diffuse through the alloy diaphragm and are dissolved into the molten salt as RE ions at the side of the cathode room. Finally, RE metals are deposited on the cathode and collected. Almost all the impurities are supposed to remain in the anode room as anode slime or deposits on the alloy diaphragm.

As the first step to apply this molten salt electrochemical process to fluoride melts, the present study focused on the Nd-Ni alloy formation in molten LiF-CaF$_2$. So far, Nourry _et al._ have reported the Nd-Ni alloy formation in molten LiF-CaF$_2$ at 1073-1223 K (3). However, the alloy phases have not been identified by XRD. Moreover, the

formation potential of each Nd-Ni alloy phase, which is crucial for the separation, has not been clarified. Thus, in the present study, the electrochemical formation of Nd-Ni alloys was investigated with emphasis on the XRD identification of alloy phases and the clarification of formation potentials.
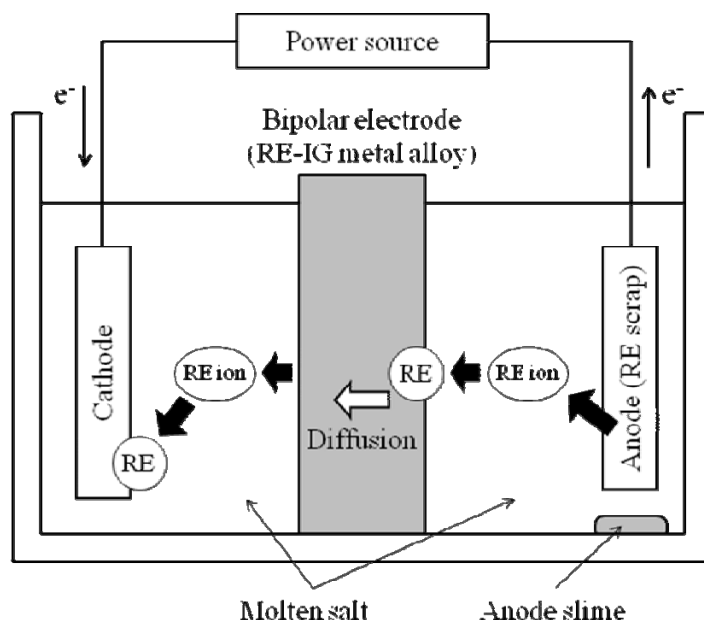

Figure 1. A new separation and recovery process of RE metals from scraps using molten salt and alloy diaphragm (1).

Experimental

LiF (99 %, Wako pure chemical Co., Ltd.) and CaF_2 (99 % up, Kojundo Chemical Laboratory Co., Ltd.) were mixed to an eutectic composition ($LiF:CaF_2$ = 80.5:19.5 mol%) and contained in a graphite or glassy carbon crucible (o.d. 90 mm x i.d. 80 mm x 120 mm, Tokai Carbon Co., Ltd.). The $LiF-CaF_2$ eutectic was kept under vacuum for more than 24 hours at 773 K to remove the absorbed water. Then, it was melted under Ar atmosphere at 1123 K. NdF_3 (99.9 %, Kojundo Chemical Laboratory Co., Ltd.) was added directly into the melts.

The working electrodes were a Ni wire (φ 1 mm), a Mo wire (φ 1 mm), or a Ni plate (8 mm x 5 mm x 0.2 mm^t). A Ni wire was used as a quasi-reference electrode and its potential was calibrated with reference to the potential of Li^+/Li dynamic electrode, which was prepared by electrodeposition of Li metal on a Ni wire. All potentials in this paper are given with reference to this Li^+/Li potential. The counter electrode was a glassy carbon rod (φ 5 mm x 50 mm, Tokai Carbon Co., Ltd.). The electrochemical measurement system (HZ3000, Hokuto Denko Corp.) connected to a personal computer was used for the measurement.

Alloy samples prepared by potentiostatic electrolysis were covered with solidified fluoride salts. Before being subjected to instrumental analysis, the salts were removed by either mechanical scraping or washing in LiCl-KCl molten salt. The alloy phase was

identified by XRD (Ultima IV, Rigaku Corporation) using Cu-Kα line (λ=0.15418 nm) at 40 kV and 40 mA. Microscopic cross-section observation of the sample was conducted by SEM using S-2600H (HITACHI Co., Ltd) or VE-8800 (KEYENCE Corp.). The compositions of the samples were analyzed by EDX using E-MAX ENERGY EX-200 (Horiba Co., Ltd.) or EDAX Genesis APEX2 (AMETEK Co., Ltd.).

Results and Discussion

Cyclic voltammetry

According to the phase diagram of Nd-Ni system (4), as shown in Figure 2, there are four intermetallic compounds: $NdNi_2$, $NdNi_3$, Nd_2Ni_7 and $NdNi_5$ at 1123 K. It is expected that these Nd-Ni alloys are formed electrochemically.
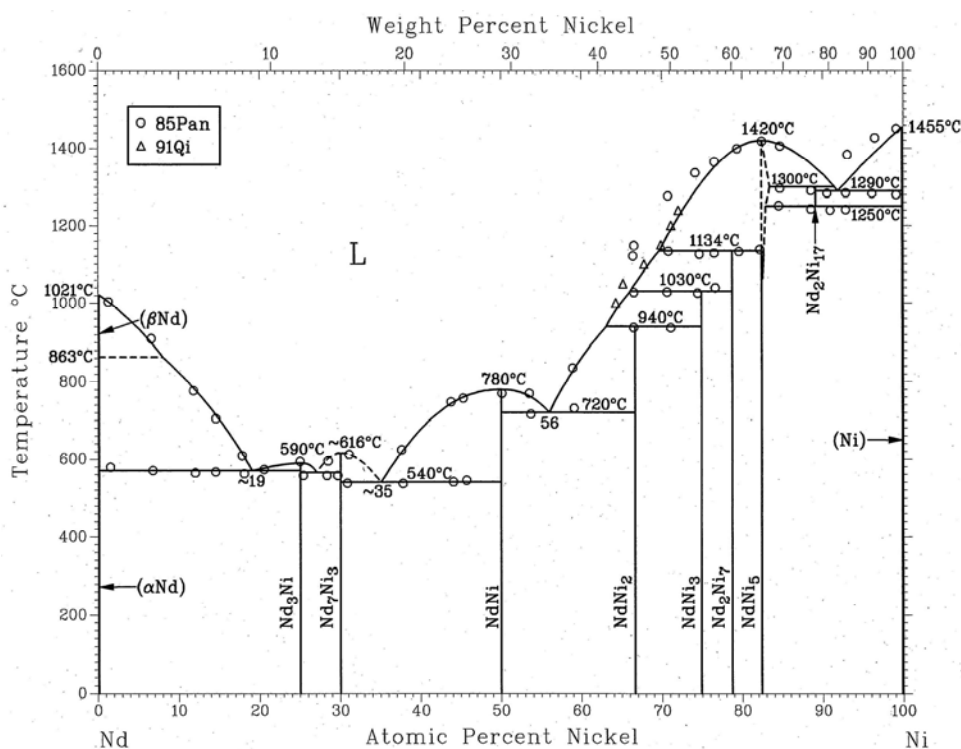

Figure 2. A binary phase diagram of the Nd-Ni system (4).

In this study, a Mo electrode was often used to compare with a Ni electrode, because no alloys exist in the binary Mo-Nd phase diagram at 1123 K (5). Before adding NdF_3, cyclic voltammetry was performed for Ni and Mo electrodes in a molten $LiF-CaF_2$ system at 1123 K. Solid curve and broken curve in Figure 3 show the obtained voltammograms for Ni and Mo electrodes, respectively. For both electrodes, a pair of sharp redox peaks are observed around 0 V (vs. Li^+/Li), which corresponds to the deposition and dissolution of lithium metal (3). For the Ni electrode, a small anodic peak is also observed at 0.2 V on the positive sweep. This anodic current is interpreted as the dissolution of Ca from Ca-Ni alloys, considering the reported binary Ca-Ni phase diagram (5).
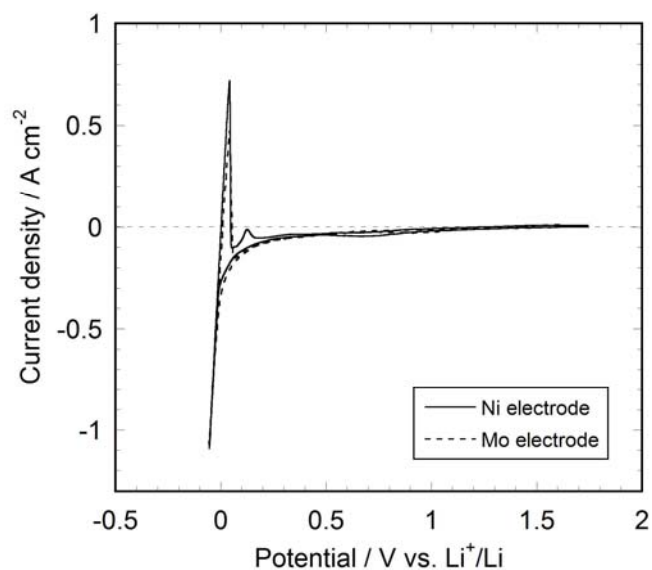
Figure 3. Cyclic voltammograms for Ni and Mo electrodes in a molten LiF-CaF$_2$ system at 1123 K. Scan rate: 0.01 V s^{-1}.

Figure 4 compares the cyclic voltammograms for Ni and Mo wire electrodes in a molten LiF-CaF$_2$-NdF$_3$ (0.30 mol%) system at 1123 K. For both Ni and Mo electrodes, new peaks are observed besides the sharp redox peaks assigned to the deposition and dissolution of lithium metal. For the Mo electrode, a cathodic current rises from 0.2 V, which is interpreted as the deposition of Nd metal. On the other hand, for the Ni electrode, cathodic current is observed from 0.7 V, suggesting the formation of Nd-Ni alloys. On the positive sweep, several anodic peaks/shoulders are observed, which are possibly caused by the dissolution of Nd from different Nd-Ni alloy phases.
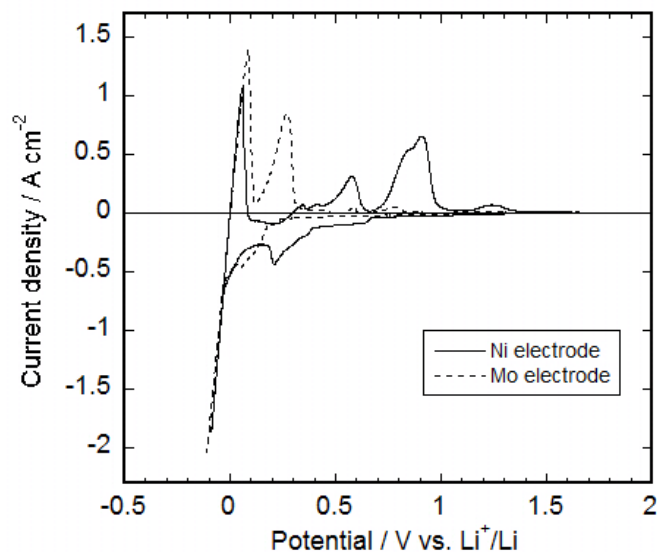

Figure 4. Cyclic voltammograms for Ni and Mo electrodes in a molten LiF-CaF$_2$-NdF$_3$ (0.30 mol%) system at 1123 K. Scan rate: 0.1 V s^{-1}.

Open-circuit potentiometry

According to our previous study, open-circuit potentiometry is more suitable for a determination of the formation potential of RE-Ni alloys (2,6). Firstly, in order to determine the Nd(III)/Nd potential, the measurement was conducted for a Mo electrode in molten $LiF-CaF_2-NdF_3$ (0.30 mol%) at 1123 K. Figure 5 shows the transient curve of open-circuit potential after galvanostatic electrolysis at -1.8 A cm^{-2} for 3 seconds. The inset shows the enlarged figure describing the potential transient in the beginning. After maintaining 0 V for 10 seconds, the electrode potential shifts and stays at 0.18 V for 20 seconds. Since Mo does not form alloy with Nd, the observed potential of 0.18 V is regarded as the Nd(III)/Nd potential.
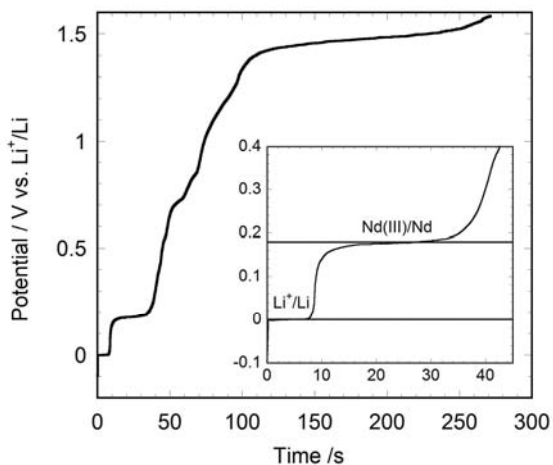

Figure 5. An open-circuit potentiogram for a Mo electrode after galvanostatic electrolysis at -1.8 A cm^{-2} for 3 s in molten $LiF-CaF_2-NdF_3$ (0.30 mol%) at 1123 K.

Secondly, open-circuit potentiometry was carried out for a Ni electrode after galvanostatic electrolysis at -0.09 A cm^{-2} for 100 s in the same melt. As shown in Figure 6, potential plateaus are observed at 0.34, 0.42, 0.49, 0.73, 0.79, 1.03 and 1.27 V. These potential plateaus possibly correspond to different coexisting Nd-Ni phases, respectively.
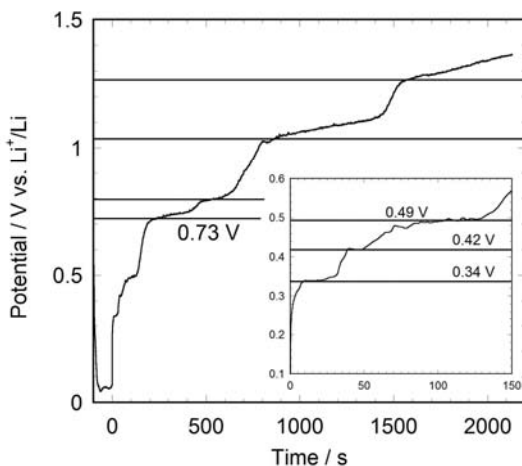

Figure 6. An open-circuit potentiogram for a Ni electrode after galvanostatic electrolysis at -0.09 A cm^{-2} for 100 s in molten $LiF-CaF_2-NdF_3$ (0.30 mol%) at 1123 K.

Preparation of Nd-Ni alloys and their characterization

To prepare an alloy sample, potentiostatic electrolysis was conducted for a Ni plate electrode at 0.15 V for 75 minutes. Figure 7 shows (a) a cross-sectional SEM image and (b) a powder XRD pattern of the sample. From the SEM image, it is found that the whole Ni disk (0.2 mm in thickness) was transformed to a Nd-Ni alloy layer. According to the powder XRD pattern, it is revealed that the alloy is a mixture of the dominant $NdNi_2$ phase and the minor $NdNi_3$ phase. Here, the calculated XRD patterns of $NdNi_2$ and $NdNi_3$ were obtained by PowderCell program, because only crystallographic parameters are available for these phases. Although the electrolysis potential of 0.15 V was more negative than Nd(III)/Nd potential, the existence of Nd metal or Nd-Ni liquid alloy was not observed in the sample, suggesting that the alloying reaction was not completed. It was found, however, that almost the whole portion of the Ni plate can be transformed to $NdNi_2$ by the present electrolysis condition.
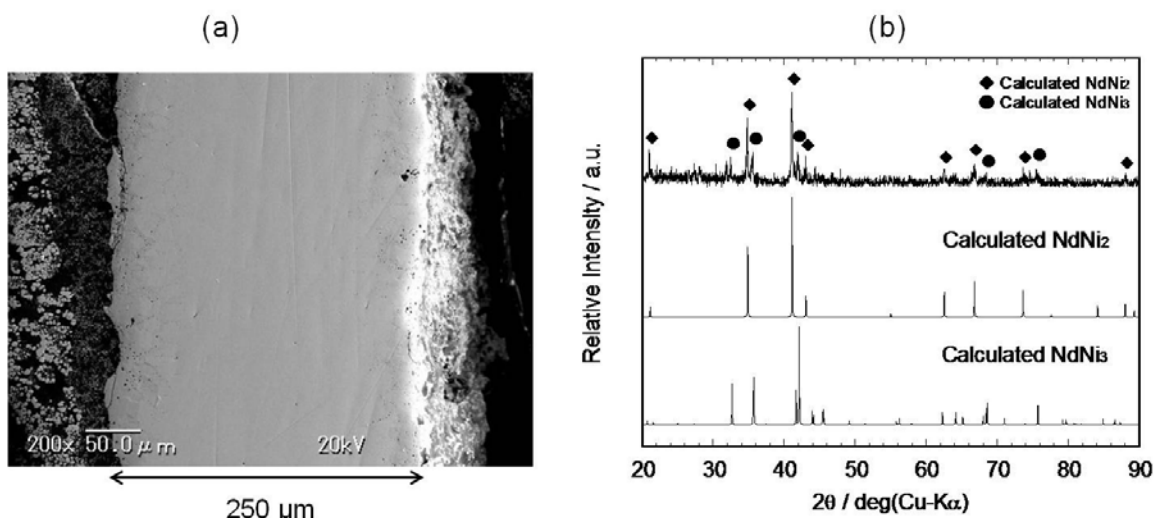

Figure 7. (a) A cross-sectional SEM image and (b) a powder XRD pattern of the sample prepared by potentiostatic electrolysis of a Ni electrode at 0.15 V for 75 minutes in molten $LiF-CaF_2-NdF_3$ (0.30 mol%) at 1123 K.

In our previous study on RE-Ni alloy formation in molten chlorides, the following phenomenon was always observed (2,7,8). When the starting electrode is Ni, the formation rates of the RE-poor phases such as $RENi_3$ and $RENi_5$ are very slow. However, when the RE-rich alloy such as $RENi_2$ is used as the starting electrode and the anodic dissolution of RE is conducted, the formation rates of the RE-poor phases become considerably high. In the present study, therefore, the $NdNi_2$ electrodes were prepared by potentiostatic electrolysis at 0.15 V for 75 minutes. Then, anodic dissolution of Nd was performed at 0.35 and 0.60 V.

The sample electrolyzed at 0.35 V for 75 minutes was found to be still a mixture of $NdNi_2$ phase and the $NdNi_3$ phase. However, relative intensities for $NdNi_3$ became larger than those for $NdNi_2$, suggesting that the equilibrium phase at 0.35 V is $NdNi_3$.

Figure 8 shows (a) a cross-sectional SEM image and (b) a powder XRD pattern of the sample prepared at 0.60 V for 50 minutes. Many fine pores are observed in the SEM image, which is explained by the dissolution of Nd from the original $NdNi_2$. By EDX analysis, its composition was found to be Nd:Ni=18:82 at.% in almost all area of the cross-section, suggesting that the alloy phase is $NdNi_5$. The powder XRD pattern clearly indicates that the $NdNi_2$ was completely transformed to $NdNi_5$.
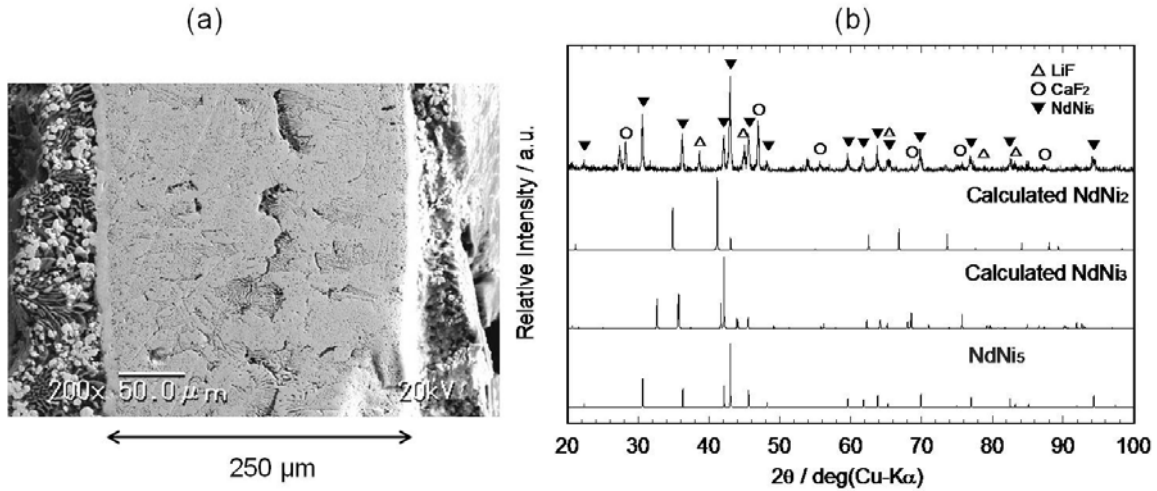

Figure 8. (a) A cross-sectional SEM image and (b) a powder XRD pattern of the sample prepared by potentiostatic electrolysis of an $NdNi_2$ electrode at 0.60 V for 50 minutes in molten $LiF-CaF_2-NdF_3$ (0.30 mol%) at 1123 K.

From the results stated above, the potential plateau at 0.34 V is considered to correspond to:

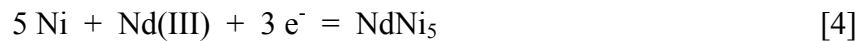$$2\ NdNi_3\ +\ Nd(III)\ +\ 3\ e^-\ =\ 3\ NdNi_2 \qquad [1]$$

Considering the number of alloy phases, though the XRD evidence has not been obtained, the plateau at 0.42 V may correspond to the equilibrium reaction.

$$3\ Nd_2Ni_7\ +\ Nd(III)\ +\ 3\ e^-\ =\ 7\ NdNi_3 \qquad [2]$$
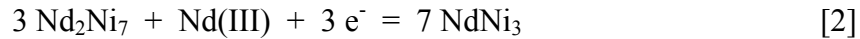
Then, according to the XRD data in Figure 8-b, the plateau at 0.49 V is interpreted as:

$$7/3\ NdNi_5\ +\ Nd(III)\ +\ 3\ e^-\ =\ 5/3\ Nd_2Ni_7 \qquad [3]$$
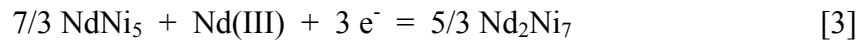
The plateau at 0.73 V would correspond to:

$$5\ Ni\ +\ Nd(III)\ +\ 3\ e^-\ =\ NdNi_5 \qquad [4]$$

Although the reason for other plateaus at 0.79, 1.03 and 1.27 V has not been clarified, they might have appeared due to the reactions of oxide formation.

Conclusions

The electrochemical formation of Nd-Ni alloys was investigated in a molten LiF-CaF$_2$-NdF$_3$ (0.30 mol%) system at 1123 K. The results obtained through this study are summarize as follows:

1. The potential of Nd(III)/Nd is 0.18 V vs. Li$^+$/Li in this system.
2. An open-circuit potentiogram obtained after galvanostatic electrolysis of a Ni electrode at -0.09 A cm^{-2} for 100 s exhibited potential plateaus at 0.34, 0.42, 0.49 and 0.73 V, suggesting the formation of coexisting Nd-Ni phases.
3. The cross-sectional SEM and powder XRD analysis revealed that the whole electrode becomes almost NdNi$_2$ phase by electrolysis of a 0.2 mm-thick Ni plate at 0.15 V vs. Li$^+$/Li for 75 minutes.
4. The formed NdNi$_2$ electrodes were transformed to other phases such as NdNi$_3$ and NdNi$_5$ by potentiostatic anodic dissolution of Nd. The existences of NdNi$_3$ and NdNi$_5$ were confirmed by powder XRD analysis.
5. The formation reaction of Nd-Ni alloys and the corresponding potential have been determined.

References

1. T. Oishi, H. Konishi, T. Nohira, M. Tanaka and T. Usui, *Kagaku Kogaku Ronbunshu*, **36**, 299 (2010). (in Japanese)
2. H. Konishi, T. Nohira and Y. Ito, *J. Electrochem. Soc.*, **148**, C506 (2001).
3. C. Nourry, L. Massot, P. Chamelot and P. Taxil, *J. New Mat. Electrochem. Systems*, **10**, 117 (2007).
4. H. Okamoto, *J. Phase Equilibria*, **13**, 218 (1992).
5. T. B. Massalski, in *Binary Alloy Phase Diagrams*, ASM International (1990).
6. H. Konishi, T. Nishikiori, T. Nohira and Y. Ito, *Electrochimica Acta*, **48**, 1403 (2003).
7. T. Iida, T. Nohira and Y. Ito, *Electrochimica Acta*, **46**, 2537 (2001).
8. T. Nohira, H. Kambara, K. Amezawa and Y. Ito, *J. Electrochem. Soc.*, **152**, C183 (2005).